

Semiclassical Analysis of Tunneling in Graphene under Nonuniform Electrostatic and Magnetic Fields

Maria V. Perel

Department of Higher Mathematics and Mathematical Physics,
St Petersburg State University,
7/9 Universitetskaya nab., St Petersburg 199034, Russian Federation

E-mail: m.perel@spbu.ru

Keywords: Dirac equation; semiclassical analysis; nonadiabatic transitions; quantum tunnelling; graphene; transfer matrix; Fabry–Pérot resonances.

Abstract

We develop a semiclassical theory of tunnelling of Dirac fermions through an n - p - n junction in monolayer graphene subjected to a perpendicular magnetic field. Electrostatic and magnetic fields are assumed to be smooth functions of a single spatial coordinate, supported on a finite interval, vanishing outside it, and thus ensuring asymptotically free states. In contrast to earlier studies restricted to constant magnetic fields and exactly solvable electrostatic potential profiles, we consider a general electrostatic potential forming an n - p - n junction and an arbitrary magnetic field, and formulate the corresponding scattering problem. Within the semiclassical approximation, and under an additional assumption on the incidence angle, the problem reduces to a connection problem for a pair of coalescing turning points, treated using results from our earlier work. We obtain explicit expressions for the reflection and transmission coefficients, including their phases, as functions of energy and incidence angle. Furthermore, we derive semiclassical conditions for Fabry–Pérot resonances and “magic” angles, and analyse the resulting interference pattern. Numerical results demonstrate the angular dependence of transmission induced by the magnetic field.

1 Introduction

The ability to control the transport of charge carriers (electrons and holes) in graphene using external electromagnetic fields is crucial for the development of electronic devices. Owing to weak particle–particle interactions, the behaviour of individual carriers can be described within a single-particle framework [1, 2, 3, 4, 5, 6, 7]. At low energies, charge carriers obey a two-dimensional massless Dirac equation with a two-component spinor structure [3, 5], neglecting intervalley scattering. External electrostatic and magnetostatic fields enter this description through scalar and vector potentials.

The study of charge-carrier dynamics in electrostatic potentials led to the discovery of Klein tunnelling [8, 7], named by analogy with the relativistic effect [9]: Charge carriers incident normally on a one-dimensional potential barrier are transmitted with unit probability, regardless of the barrier height. This implies that purely electrostatic fields cannot confine carriers along their direction of variation. For oblique incidence, however, partial reflection occurs. This regime has been analysed for several exactly solvable potentials, including linear profiles forming n - p junctions [10], as well as trapezoidal and hyperbolic-secant barriers [11, 12]. Arbitrary smooth potentials generating n - p - n junctions were treated asymptotically in [13, 14] for massless fermions and in [15] for massive fermions. These studies also demonstrated the emergence of Fabry–Pérot resonances due to multiple reflections at the interfaces.

In contrast, inhomogeneous magnetic barriers without electrostatic potentials were considered in [16, 17], and methods for generating inhomogeneous magnetic fields were discussed in [18].

Some qualitative features of carrier transport in the presence of both electrostatic and magnetic fields were discussed in [10, 19, 20, 21]. Suppression of transport in n - p - n junctions by magnetic fields was predicted in [10]: the curvature of carrier trajectories effectively modifies the incidence angle at

the interfaces, thereby reducing transmission. In [19, 20], transmission coefficients for n - p junctions in constant electric and magnetic fields were obtained using Lorentz transformations, revealing two distinct regimes: weak magnetic fields, which perturb tunnelling, and strong fields, which alter the Landau-level structure. Interference effects for a parabolic barrier in a constant magnetic field were analysed in [21] under the assumption that both the electrostatic potential and the vector potential are symmetric.

Quantitative analyses of carrier transport in both electric and magnetic fields have mostly focused on constant magnetic fields and potentials that allow exact solutions, which are often expressed in analytically involved forms and require further numerical evaluation. Electron transmission through rectangular and double barriers was studied in [22], whereas triangular barriers were investigated numerically in [23]. Similar problems have also been considered in other Dirac materials [24]. Transport in weak magnetic fields and stepped potentials was analysed in [25].

Despite this progress, the scattering problem for Dirac fermions in the presence of simultaneously varying electrostatic and magnetic fields of arbitrary smooth profiles—forming n - p and p - n junctions and vanishing outside a finite interval—has not yet been systematically addressed. To our knowledge, explicit semiclassical expressions for both the amplitudes and phases of the scattering coefficients for such combined fields are not available.

In this paper, we present a study of stationary transport of two-dimensional Dirac fermions in graphene through smooth electrostatic and magnetic barriers coexisting within the same spatial region. No symmetry assumptions are imposed. We adopt a gauge in which both the scalar and vector potentials depend solely on a single spatial coordinate. The electrostatic potential forms a n - p - n junction with monotonically increasing and decreasing regions separated by a plateau, while the magnetic field is perpendicular, weak according to the criterion of [19, 20], and features a single maximum. Outside a finite interval, both fields vanish. By solving the corresponding scattering problem, we determine both the amplitudes and phases of the reflection and transmission coefficients, providing explicit expressions suitable for qualitative and quantitative analysis of carrier transport in these barrier configurations.

Our approach is based on a semiclassical construction of transfer matrices associated with individual n - p and p - n interfaces. The scattering problem for the Dirac equation is closely related to the Landau-Zener problem, as noted in [21, 11]. In this analogy, the spatial coordinate replaces time, while the spatially varying potential produces an avoided crossing of the real-valued, position-dependent longitudinal momentum, with a gap separating the electron and hole branches. However, significant differences nevertheless emerge. The Dirac equation can be expressed as a Schrödinger-type equation with a non-selfadjoint matrix Hamiltonian that admits a specific factorization. Similar formulations arise in wave-propagation problems, including electromagnetic waves in the Earth-ionosphere waveguide [26] and elastic waves in inhomogeneous waveguides [27]. A general framework for such scattering problems was developed in [28] and we apply here the general results to the case of Dirac fermions.

The phase of the reflection coefficient plays a crucial role in determining interference effects in the n - p - n structure. In particular, it enables us to derive explicit semiclassical conditions for Fabry-Pérot resonances as well as “magic” angles corresponding to enhanced transmission. In the absence of a magnetic field, our results reduce to previously obtained semiclassical expressions [13, 14].

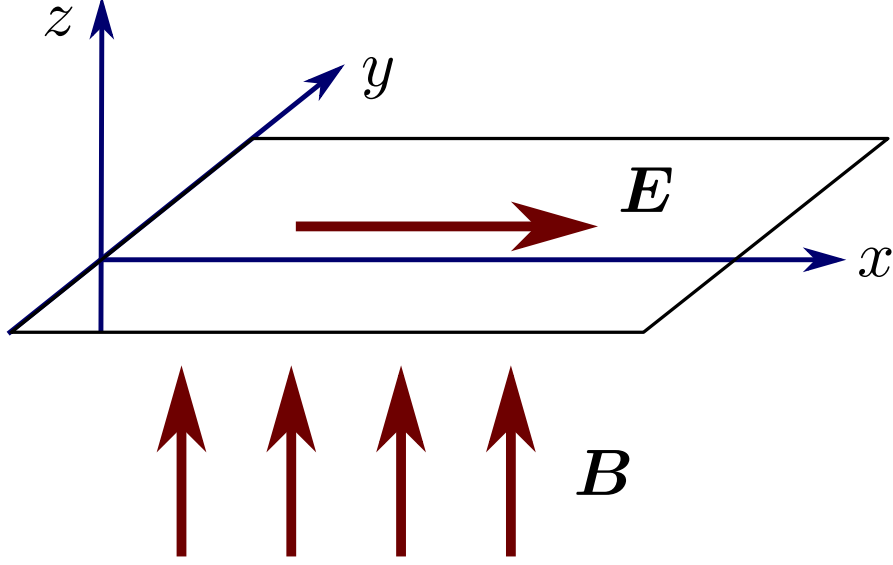
We further predict characteristic restructuring of the interference pattern at energies and angles corresponding to perfect transmission through individual interfaces. Finally, numerical examples are presented to illustrate the significant influence of the magnetic field on carrier transmission through the junction.

2 Model and Basic Equations

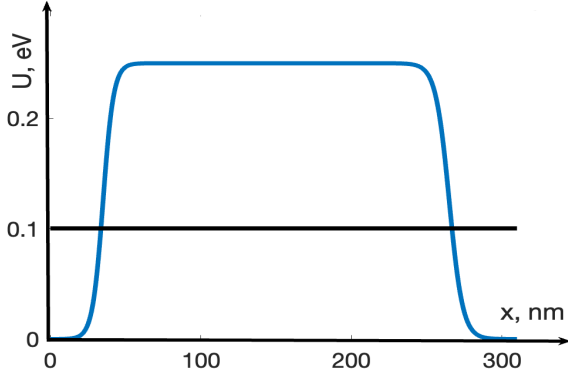
We consider a graphene monolayer subjected to external static electric and magnetic fields, \mathbf{E} and \mathbf{B} , respectively. The field configuration is shown in figure 1. A graphene sheet lies in the (x, y) plane. The electric field is directed along the x axis (or opposite to it), while the magnetic field is perpendicular to the graphene plane. The electrostatic potential varies within the interval $x_* < x < x_{**}$. Both fields depend smoothly on x and are uniform in the y direction.

The fields are described by a scalar potential $U(x)$ and a vector potential $\mathbf{A}(x)$, defined up to a gauge transformation. Choosing the Landau gauge [29],

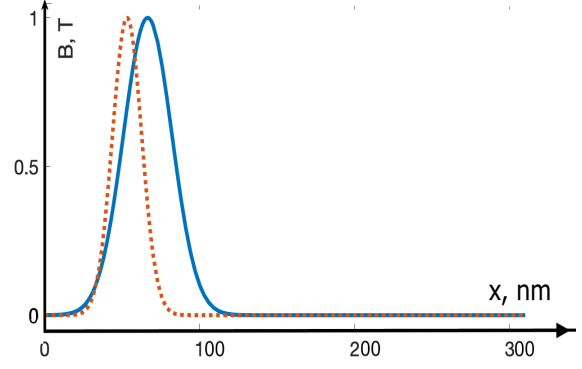
$$\mathbf{A} = (0, A_y(x), 0), \tag{1}$$



(a) Geometry and field configuration.



(b) Electrostatic barrier $U(x)$.



(c) Magnetic-field profiles $B(x)$.

Figure 1: Schematic of Klein tunnelling in graphene under external fields. The horizontal line indicates the carrier energy \mathcal{E} .

the vector potential is fixed up to an additive constant,

$$A_y(x) = A_y(0) + \int_0^x B(\tilde{x}) d\tilde{x}. \quad (2)$$

Any other gauge choice would introduce an explicit y -dependence of A_y . The corresponding fields read

$$\mathbf{B} = \nabla \times \mathbf{A}, \quad \mathbf{E} = -\nabla U(x), \quad (3)$$

where $\mathbf{B} = (0, 0, B(x))$.

The dynamics of a single charge carrier is governed by the $(2+1)$ -dimensional Dirac equation [3],

$$i\hbar \frac{\partial}{\partial t} \Upsilon = \hat{H}(\hat{\mathbf{p}}, \mathbf{r}) \Upsilon, \quad \mathbf{r} = (x, y), \quad (4)$$

with the Hamiltonian

$$\hat{H} = v_F \boldsymbol{\sigma} \cdot (\hat{\mathbf{p}} + e\mathbf{A}(\mathbf{r})) + U(\mathbf{r}), \quad (5)$$

where $\hat{\mathbf{p}} = -i\hbar\nabla$, v_F is the Fermi velocity, and e is the electron charge. The Pauli matrices are

$$\sigma_x = \begin{pmatrix} 0 & 1 \\ 1 & 0 \end{pmatrix}, \quad \sigma_y = \begin{pmatrix} 0 & -i \\ i & 0 \end{pmatrix}, \quad (6)$$

and $\boldsymbol{\sigma} = (\sigma_x, \sigma_y)$. The Hamiltonian (5) describes carriers near the K point of the graphene band structure. We restrict ourselves to weak magnetic fields, defined by the condition

$$|v_F^{-1}U'(x)| > e|B(x)|. \quad (7)$$

For a locally homogeneous system with the same values of $U'(x)$ and $B(x)$, condition (7) implies that a Lorentz frame exists in which the magnetic field vanishes [19]. In this case, the electric field dominates over the magnetic field in the semiclassical dynamics. This condition must hold at the turning points defined by $\mathcal{E} = U(x)$. The carrier energy \mathcal{E} lies in the interval $(0, \max U)$ and is assumed not to be close to $\max U$.

We seek stationary states of energy \mathcal{E} in the form

$$\Upsilon(\mathbf{r}, t) = e^{i(p_y y - \mathcal{E}t)/\hbar} \Psi(x), \quad (8)$$

where p_y is the conserved transverse momentum. Substitution into the Dirac equation yields a one-dimensional system,

$$-i\hbar\sigma_x \frac{d\Psi}{dx} = \hat{\mathcal{K}}(x)\Psi, \quad \hat{\mathcal{K}}(x) = \begin{pmatrix} \mathcal{E} - U(x) & i\mathcal{P} \\ -i\mathcal{P} & \mathcal{E} - U(x) \end{pmatrix}, \quad (9)$$

with

$$\mathcal{P} = p_y + eA_y(x). \quad (10)$$

We introduce dimensionless variables according to

$$x = \frac{\check{x}}{\check{l}}, \quad \mathcal{E} = \frac{\check{\mathcal{E}}}{\check{v}_F \check{p}_0}, \quad U = \frac{\check{U}}{\check{v}_F \check{p}_0}, \quad A_y = \frac{\check{e}\check{A}_y}{\check{p}_0}, \quad p_y = \frac{\check{p}_y}{\check{p}_0}, \quad \hbar = \frac{\check{\hbar}}{\check{p}_0 \check{l}}. \quad (11)$$

Quantities with a check denote dimensional variables. We adopt the values $\check{v}_F = 10^6 \text{ ms}^{-1}$, $\check{\hbar} = 6.6 \times 10^{-16} \text{ eV}\cdot\text{s}$, and $\check{e} = 1 \text{ eV/V}$.

As a representative example, we consider an electrostatic barrier with $\max \check{U} = 250 \text{ meV}$, $\check{l}_{n-p} = 70 \text{ nm}$, $\check{l}_{p-n} = 90 \text{ nm}$, and a constant-potential region of length $\check{l}_{\text{const}} = 150 \text{ nm}$, as in [14]. Choosing $\check{\mathcal{E}}_0 - \check{U}_0 = 0.1 \text{ eV}$ and $\check{l} = 70 \text{ nm}$, we define

$$\check{p}_0 = (\check{\mathcal{E}}_0 - \check{U}_0)\check{v}_F^{-1},$$

which gives

$$\hbar = \frac{\check{\hbar}\check{v}_F}{(\check{\mathcal{E}}_0 - \check{U}_0)\check{l}} \approx 0.1. \quad (12)$$

In what follows, all dimensionless variables and their derivatives are assumed to be of order unity. We set $e = v_F = 1$ and omit them hereafter. The small parameter $\hbar \ll 1$ serves as the semiclassical expansion parameter.

3 Semiclassical Approach

We solve equation (9) using the semiclassical (WKB) approximation [30, 31]. In this framework, the solution is expressed in terms of the local classical momentum. As long as the semiclassical approximation remains valid, a charge carrier follows a single classical trajectory and no scattering occurs. Scattering becomes possible only in regions where the semiclassical approximation breaks down.

Mathematically, equation (9) is a system of ordinary differential equations with a small parameter \hbar multiplying the derivative. Semiclassical methods for such systems are well established [32, 33]. In the absence of a magnetic field, this equation was analyzed asymptotically in [13, 14, 15] by reducing it to a second-order scalar equation. In contrast, we treat the first-order system directly, which allows for a transparent inclusion of the magnetic field.

We employ the semiclassical (WKB) ansatz

$$\Psi(x) = \exp\left[\frac{i}{\hbar} \int^x \beta(s) ds\right] \sum_{m=0}^{\infty} \hbar^m \Phi^{(m)}(x), \quad (13)$$

where $\beta(x)$ and $\Phi^{(m)}(x)$ are sufficiently smooth functions of x . Substitution of (13) into (9) yields a hierarchy of algebraic equations.

The zeroth-order equation gives

$$\Phi_j^{(0)}(x) = C_j^{(0)}(x) \varphi_j(x), \quad (14)$$

where $\varphi_j(x)$ satisfies

$$\widehat{\mathcal{K}}(x) \varphi_j(x) = \beta_j(x) \sigma_x \varphi_j(x). \quad (15)$$

The eigenvalues $\beta_j(x)$ are given by appropriate branches of

$$\beta(x) = \sqrt{(\mathcal{E} - U(x))^2 - \mathcal{P}^2(x)}, \quad (16)$$

with the choice of branches specified below. They represent the longitudinal momentum, i.e. the classical momentum along the x -direction.

Regions where $\beta(x)$ is real (imaginary) correspond to classically allowed (forbidden) motion. Turning (degeneracy) points \varkappa for linear systems of ordinary differential equations are defined as the coordinates x at which two eigenvalues β coincide, see for example [32]. For system (9), the turning points satisfy the condition $\beta(\varkappa) = 0$.

If $\mathcal{P}(x) = 0$, there is a single doubly degenerate turning point $\varkappa_{\mathcal{E}}$ determined by

$$\mathcal{E} = U(\varkappa_{\mathcal{E}}), \quad (17)$$

which corresponds to Klein tunnelling [8].

For $\mathcal{P}(\varkappa_{\mathcal{E}}) \neq 0$, this degeneracy is lifted, and the turning point splits into two simple turning points $\varkappa_- < \varkappa_+$ defined by

$$|\mathcal{E} - U(\varkappa_{\pm})| = |\mathcal{P}(\varkappa_{\pm})|. \quad (18)$$

In the classically allowed regions, the eigenvalues are labeled as follows:

$$\beta_1(x) = -\beta_2(x), \quad \beta_2(x) = \begin{cases} |\beta(x)|, & x > \varkappa_+, \\ -|\beta(x)|, & x < \varkappa_-. \end{cases} \quad (19)$$

The corresponding eigenvectors take the form

$$\varphi_j(x) = \begin{pmatrix} \beta_j(x) - i\mathcal{P}(x) \\ \mathcal{E} - U(x) \end{pmatrix}. \quad (20)$$

The solvability condition for the first-order correction $\Phi_j^{(1)}(x)$ leads to

$$C_j^{(0)}(x) = \frac{\mathcal{A}_j}{\sqrt{|N_j(x)|}} \exp \left[-i \int_a^x \text{Im} S_j(x') dx' \right], \quad (21)$$

where

$$S_j(x) = \frac{(\varphi_j, \sigma_x \varphi_j')}{(\varphi_j, \sigma_x \varphi_j)}, \quad N_j(x) = (\varphi_j, \sigma_x \varphi_j) = 2\beta_j(x)(\mathcal{E} - U(x)). \quad (22)$$

Evaluating the integral in (21) yields the leading-order semiclassical solution

$$\Psi_j(x) \approx \frac{\varphi_j(x)}{\sqrt{|N_j(x)|}} \exp \left\{ \frac{i}{\hbar} \int_a^x \beta_j(x') dx' - i\gamma_j(x) + i\gamma_j(a) \right\}, \quad (23)$$

where the Berry phase is given by

$$\gamma_j(x) = -\frac{1}{2} \arcsin \frac{\mathcal{P}(x)}{|\mathcal{E} - U(x)|} \text{sgn} \beta_j(x). \quad (24)$$

Choosing the lower limit $a = \varkappa_c$ as the nearest turning point $\varkappa_c = \varkappa_{\pm}$, we obtain

$$\begin{aligned} \Psi_j^c(x) &= \frac{\varphi_j(x)}{\sqrt{|2\beta_j(x)(\mathcal{E} - U(x))|}} \\ &\times \exp \left[i \text{sgn} \beta_j(x) \left(\frac{1}{\hbar} \int_{\varkappa_c}^x |\beta_j(x')| dx' + \frac{1}{2} \arcsin \frac{\mathcal{P}(x)}{|\mathcal{E} - U(x)|} \right) + i\gamma_j(\varkappa_c) \right] \end{aligned} \quad (25)$$

Here

$$c = \pm, \quad \gamma_j(\kappa_c) = -\text{sgn}\beta_j(x) \chi_\mathcal{E}, \quad \kappa_c = \kappa_\pm, \quad \chi_\mathcal{E} = \frac{\pi}{4} \text{sgn}\mathcal{P}(\kappa_\mathcal{E}), \quad (26)$$

which results from the assumption of weak B and the relations

$$\begin{aligned} \kappa_c - \kappa_\mathcal{E} &\approx \pm \frac{p_y + A_y(\kappa_\mathcal{E})}{U'(\kappa_\mathcal{E}) \mp B(\kappa_\mathcal{E})}, \\ \mathcal{P}(\kappa_c) &\approx \mathcal{P}(\kappa_\mathcal{E}) + B(\kappa_\mathcal{E}) (\kappa_c - \kappa_\mathcal{E}) = \mathcal{P}(\kappa_\mathcal{E}) \frac{U'(\kappa_\mathcal{E})}{U'(\kappa_\mathcal{E}) \mp B(\kappa_\mathcal{E})}. \end{aligned} \quad (27)$$

The approximation (25) breaks down at the turning points $x = \kappa_\pm$, where $\beta_j(x)$ vanishes. A general solution can be written as

$$\Psi(x) \approx \begin{cases} k_1^- \Psi_1^-(x) + k_2^- \Psi_2^-(x), & x \ll \kappa_-, \\ k_1^+ \Psi_1^+(x) + k_2^+ \Psi_2^+(x), & x \gg \kappa_+, \end{cases} \quad (28)$$

which defines the transfer matrix \mathcal{T} :

$$\begin{pmatrix} k_1^+ \\ k_2^+ \end{pmatrix} = \mathcal{T} \begin{pmatrix} k_1^- \\ k_2^- \end{pmatrix}. \quad (29)$$

4 Scattering Problem

We consider scattering of a charge carrier by an electrostatic potential barrier in the presence of an external magnetic field (see figure 2).

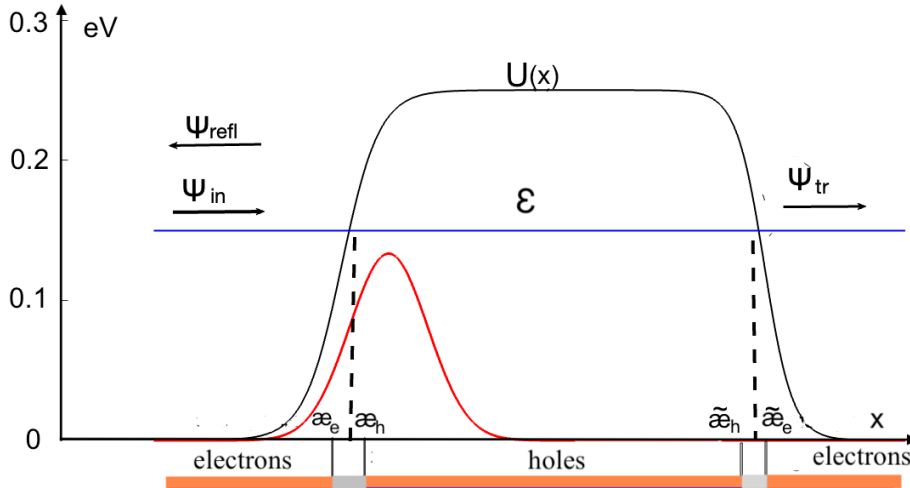


Figure 2: Charge carrier scattering at a potential barrier $U(x)$ in a spatially varying magnetic field $B(x)$. Horizontal line: carrier energy \mathcal{E} . Incoming, reflected, and transmitted waves are Ψ_{in} , Ψ_{refl} , and Ψ_{tr} . Dashed vertical lines indicate $x = \kappa_\mathcal{E}$, defined by $\mathcal{E} = U(\kappa_\mathcal{E})$. Small ticks indicate the turning (degeneracy) points κ_e , κ_h , $\tilde{\kappa}_h$, and $\tilde{\kappa}_e$, which delimit the interfaces between classically allowed and forbidden regions. The central allowed region is hole-like, whereas the outer allowed regions are electron-like.

The charge carrier is incident on the barrier at an angle θ with energy \mathcal{E} . We assume that the electromagnetic field vanishes for $x \leq x_*$, and choose the gauge $A_y(x_*) = 0$, which affects the wave function only through an irrelevant y -dependent phase. From (16), at $x = x_*$ one has

$$\beta^2(x_*) + p_y^2 = \mathcal{E}^2, \quad (30)$$

so that

$$\beta(x_*) = \mathcal{E} \cos \theta, \quad p_y = \mathcal{E} \sin \theta. \quad (31)$$

For $x > x_*$ the function $\beta(x)$ is determined by equation (16). We also assume that fields vanish for $x \geq x_{**}$.

The wave function is written as

$$\Psi(x) = \begin{cases} \Psi_{\text{in}}(x) + r_{\text{n-p-n}} \Psi_{\text{refl}}(x), & x \leq x_*, \\ t_{\text{n-p-n}} \Psi_{\text{tr}}(x), & x \geq x_{**}. \end{cases} \quad (32)$$

Here Ψ_{in} and Ψ_{refl} describe incoming and reflected waves to the left of the barrier, while Ψ_{tr} corresponds to the transmitted wave. We denote the transmitted and reflected coefficients by $t_{\text{n-p-n}}$ and $r_{\text{n-p-n}}$, respectively.

To construct the transfer matrix, we distinguish classically allowed and forbidden regions. For a given energy \mathcal{E} , equation (17) has two solutions, $\varkappa_{\mathcal{E}}$ and $\tilde{\varkappa}_{\mathcal{E}}$, corresponding to increasing and decreasing parts of the potential, respectively. Forbidden regions arise in the intervals $\varkappa_- < x < \varkappa_+$ and $\tilde{\varkappa}_- < x < \tilde{\varkappa}_+$. The semiclassical solutions Ψ_j^{ε} and $\tilde{\Psi}_j^{\varepsilon}$ are defined in the vicinity of the corresponding forbidden regions. The carrier is an electron when $\mathcal{E} > U(x)$ and a hole when $\mathcal{E} < U(x)$, therefore

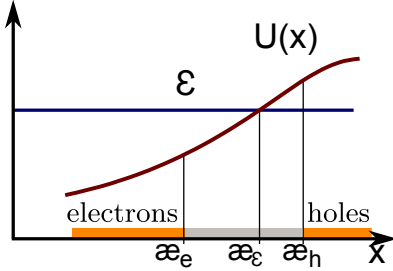


Figure 3: Turning points \varkappa_e and \varkappa_h for electrons and holes with energy \mathcal{E} in a monotonically increasing electrostatic potential $U(x)$. The classically allowed regions are $x < \varkappa_e$ and $x > \varkappa_h$, whereas the classically forbidden region is $\varkappa_e < x < \varkappa_h$.

$$\varkappa_- \equiv \varkappa_e, \quad \varkappa_+ \equiv \varkappa_h, \quad \tilde{\varkappa}_- \equiv \tilde{\varkappa}_h, \quad \tilde{\varkappa}_+ \equiv \tilde{\varkappa}_e.$$

The direction of propagation is determined by the conserved current

$$j_x = (\Psi, \sigma_x \Psi) = \text{const}, \quad (33)$$

which yields

$$\text{sign}(j_x) = \text{sign}\left(2\beta_j(x)(\mathcal{E} - U(x))\right). \quad (34)$$

Accordingly, we label the modes by eR , eL , hR , and hL .

The correspondence between the semiclassical solutions reads

$$\Psi_1^- = \Psi_{eR}, \quad \Psi_2^- = \Psi_{eL}, \quad \Psi_1^+ = \Psi_{hR}, \quad \Psi_2^+ = \Psi_{hL}, \quad (35)$$

$$\tilde{\Psi}_1^- = \tilde{\Psi}_{hL}, \quad \tilde{\Psi}_2^- = \tilde{\Psi}_{hR}, \quad \tilde{\Psi}_1^+ = \tilde{\Psi}_{eL}, \quad \tilde{\Psi}_2^+ = \tilde{\Psi}_{eR}. \quad (36)$$

For a monotonically increasing potential, the transfer matrix $\mathcal{T}_{\text{n-p}}$ relates the expansion coefficients of a general solution $\Psi(x)$, which has the asymptotic

$$\Psi(x) \approx \begin{cases} k_{eR} \Psi_{eR}(x) + k_{eL} \Psi_{eL}(x), & x \ll \varkappa_e, \\ k_{hR} \Psi_{hR}(x) + k_{hL} \Psi_{hL}(x), & x \gg \varkappa_h \end{cases} \quad (37)$$

across the classically forbidden region between the turning points \varkappa_e and \varkappa_h :

$$\begin{pmatrix} k_{hR} \\ k_{hL} \end{pmatrix} = \mathcal{T}_{\text{n-p}} \begin{pmatrix} k_{eR} \\ k_{eL} \end{pmatrix}. \quad (38)$$

Setting

$$k_{eL} = r_{\text{n-p}}, \quad k_{eR} = 1, \quad k_{hL} = 0, \quad k_{hR} = t_{\text{n-p}}, \quad (39)$$

one finds

$$r_{\text{n-p}} = -\frac{(\mathcal{T}_{\text{n-p}})_{21}}{(\mathcal{T}_{\text{n-p}})_{22}}, \quad t_{\text{n-p}} = \frac{\det \mathcal{T}_{\text{n-p}}}{(\mathcal{T}_{\text{n-p}})_{22}}. \quad (40)$$

For a potential monotonically decreasing along x , the transfer matrix $\mathcal{T}_{p-n} = \tilde{\mathcal{T}}$ relates electron and hole coefficients via

$$\begin{pmatrix} \tilde{k}_{eL} \\ \tilde{k}_{eR} \end{pmatrix} = \mathcal{T}_{p-n} \begin{pmatrix} \tilde{k}_{hL} \\ \tilde{k}_{hR} \end{pmatrix}, \quad (41)$$

and, setting $\tilde{k}_{eL} = 0$, $\tilde{k}_{eR} = t_{p-n}$, $\tilde{k}_{hL} = r_{p-n}$, $\tilde{k}_{hR} = 1$, one finds

$$r_{p-n} = -\frac{(\mathcal{T}_{p-n})_{12}}{(\mathcal{T}_{p-n})_{11}}, \quad t_{p-n} = \frac{\det \mathcal{T}_{p-n}}{(\mathcal{T}_{p-n})_{11}}. \quad (42)$$

Propagation between the two classically forbidden regions is described by the transfer matrix

$$\mathcal{T}_{p-p} = \begin{pmatrix} 0 & e^{i\zeta} \\ e^{-i\zeta} & 0 \end{pmatrix}, \quad \zeta = \frac{1}{\hbar} \int_{\varkappa_h}^{\tilde{\varkappa}_h} |\beta(x')| dx' + \tilde{\chi}_\mathcal{E} - \chi_\mathcal{E}, \quad (43)$$

where, according to (26),

$$\tilde{\chi}_\mathcal{E} - \chi_\mathcal{E} = \frac{\pi}{4} [\text{sign } \mathcal{P}(\tilde{\varkappa}_\mathcal{E}) - \text{sign } \mathcal{P}(\varkappa_\mathcal{E})]. \quad (44)$$

The total transfer matrix through the barrier is

$$\mathcal{T}_{n-p-n} = \mathcal{T}_{p-n} \mathcal{T}_{p-p} \mathcal{T}_{n-p}. \quad (45)$$

Imposing $\tilde{k}_{eL} = 0$, $\tilde{k}_{eR} = t_{n-p-n}$, $k_{eR} = 1$, $k_{eL} = r_{n-p-n}$, we obtain

$$r_{n-p-n} = -\frac{(\mathcal{T}_{n-p-n})_{11}}{(\mathcal{T}_{n-p-n})_{12}}, \quad t_{n-p-n} = -\frac{\det \mathcal{T}_{n-p-n}}{(\mathcal{T}_{n-p-n})_{12}}. \quad (46)$$

5 Transfer Matrix Calculation

In the previous section, we demonstrated that once the transfer matrix \mathcal{T} is known, the scattering problem for the potential barriers shown in Fig. 2 can be solved. It has been noted in several works (see [19, 11]) that the equations describing charge-carrier scattering by a monotonic electrostatic barrier in graphene are closely related to those of the Landau–Zener problem. A broader class of systems encompassing the present case was analyzed in [28], where the distinction from the conventional Landau–Zener setting was discussed. Here we specialize the transfer matrix obtained in [28] to our problem. The matrix connects the simplified semiclassical solutions introduced above and differs from the original solutions by a phase factor determined explicitly below.

5.1 Reduction of the Dirac Equation to a Schrödinger-Type Equation

We rewrite the quantity $\mathcal{P}(x)$ appearing in equation (9) as

$$\mathcal{P}(x) = p_y + A_y(\varkappa_\mathcal{E}) + [A_y(x) - A_y(\varkappa_\mathcal{E})], \quad (47)$$

and assume

$$p_y + A_y(\varkappa_\mathcal{E}) = \delta \mathcal{P}_\mathcal{E}, \quad \delta \ll 1, \quad \mathcal{P}_\mathcal{E} \sim 1. \quad (48)$$

This inequality thus restricts the allowed charge-carrier incidence angles to values close to the angle of full transmission. For a single p - n junction, $\varkappa_\mathcal{E}$ should be replaced by $\tilde{\varkappa}_\mathcal{E}$.

With this decomposition, the matrix $\hat{\mathcal{K}}$ in (9) can be written as

$$\begin{aligned} \hat{\mathcal{K}}(x) &= \mathcal{K}(x) + \delta \mathcal{B}, \\ \mathcal{K}(x) &= \begin{pmatrix} U(\varkappa_\mathcal{E}) - U(x) & i[A_y(x) - A_y(\varkappa_\mathcal{E})] \\ -i[A_y(x) - A_y(\varkappa_\mathcal{E})] & U(\varkappa_\mathcal{E}) - U(x) \end{pmatrix}, \\ \mathcal{B} &= \begin{pmatrix} 0 & i\mathcal{P}_\mathcal{E} \\ -i\mathcal{P}_\mathcal{E} & 0 \end{pmatrix}. \end{aligned} \quad (49)$$

Equation (9) then reduces to

$$-i\hbar\sigma_x \frac{d\Psi(x)}{dx} = [\mathcal{K}(x) + \delta \mathcal{B}] \Psi(x). \quad (50)$$

This equation contains two small parameters: the dimensionless Planck constant \hbar and the perturbation parameter δ . Formally, it resembles a Schrödinger equation with x playing the role of time and $\mathcal{K}(x) + \delta\mathcal{B}$ acting as an effective Hamiltonian. However, the operator $\sigma_x^{-1}[\mathcal{K}(x) + \delta\mathcal{B}]$ is non-Hermitian, and $\Psi(x)$ is a two-component vector. For this reason, we refer to equation (50) as a Schrödinger-type equation. The corresponding scattering problem was analyzed in [28].

We consider the unperturbed eigenvalue problem

$$\mathcal{K}(x)\varphi_j^0(x) = \beta_j^0(x)\sigma_x\varphi_j^0(x), \quad j = 1, 2, \quad (51)$$

which has the following properties:

- The eigenvalues $\beta_1^0(x)$ and $\beta_2^0(x)$ cross at $x = \varkappa_\mathcal{E}$. In the vicinity of this point,

$$\beta_2^0(x) - \beta_1^0(x) \sim 2Q(x - \varkappa_\mathcal{E}), \quad Q > 0. \quad (52)$$

- The eigenvectors $\varphi_1^0(\varkappa_\mathcal{E})$ and $\varphi_2^0(\varkappa_\mathcal{E})$ are linearly independent.
- The eigenvalues and eigenvectors are smooth functions of x .

Following [28], we assume

$$\delta \sim \sqrt{\hbar}, \quad (53)$$

thereby neglecting study of exponentially small contributions to the scattering matrix while retaining nonadiabatic transitions.

In the vicinity of $x = \varkappa_\mathcal{E}$, the scattering problem is formulated in terms of simplified with account of (53) semiclassical solutions named $\Psi_j^{c,0}(x)$,

$$\begin{aligned} \Psi_j^{c,0}(x) &= \frac{\varphi_j^0(x)}{|N_j^0(x)|^{1/2}} \exp\left[i \int_{\varkappa_c}^x \left(\frac{\beta_j(x')}{\hbar} - \text{Im}S_j^0(x')\right) dx'\right], \\ N_j^0(x) &= (\varphi_j^0(x), \sigma_x \varphi_j^0(x)), \\ S_j^0(x) &= \frac{(\varphi_j^0(x), \sigma_x d\varphi_j^0/dx)}{N_j^0(x)}. \end{aligned} \quad (54)$$

The lower integration limit is $\varkappa_c = \varkappa_-$ or \varkappa_+ , depending on the region of x . Unlike the solutions $\Psi_j^c(x)$, the amplitude prefactor and $S_j^0(x)$ are evaluated using the simplified eigenfunctions $\varphi_j^0(x)$, whereas the phase contains the exact eigenvalues $\beta_j(x)$.

Any solution $\Psi(x)$ can be decomposed as

$$\begin{aligned} \Psi(x) &\approx k_1^{-,0}\Psi_1^{-,0} + k_2^{-,0}\Psi_2^{-,0}, & x \ll \varkappa_\mathcal{E}, \\ \Psi(x) &\approx k_1^{+,0}\Psi_1^{+,0} + k_2^{+,0}\Psi_2^{+,0}, & x \gg \varkappa_\mathcal{E}. \end{aligned} \quad (55)$$

The transfer matrix \mathcal{T}^0 is defined by

$$\begin{pmatrix} k_1^{+,0} \\ k_2^{+,0} \end{pmatrix} = \mathcal{T}^0 \begin{pmatrix} k_1^{-,0} \\ k_2^{-,0} \end{pmatrix}, \quad (56)$$

and takes the form [28]

$$\mathcal{T}^0 = \begin{pmatrix} e^{\pi|\nu|} & e^{2i\Theta_1} \sqrt{|1 - e^{2\pi|\nu|}|} \\ e^{-2i\Theta_1} \sqrt{|1 - e^{2\pi|\nu|}|} & e^{\pi|\nu|} \end{pmatrix}, \quad \det \mathcal{T}^0 = 1. \quad (57)$$

The parameter ν and the phase Θ_1 are given by

$$\nu = -i \frac{p^2}{2Q}, \quad p^2 = \frac{\mathcal{B}_{12}^{(0)} \mathcal{B}_{21}^{(0)}}{|N_1^0 N_2^0|}, \quad (58)$$

where $N_j^0 = N_j^0(\varkappa_\mathcal{E})$ and

$$\mathcal{B}_{ji}^{(0)} = (\varphi_j^0(x), \mathcal{B}(x)\varphi_i^0(x)) \Big|_{x=\varkappa_\mathcal{E}}.$$

The coefficient Q characterizes the linear behavior of the eigenvalues near $x = \varkappa_\varepsilon$, see (52).

The phase Θ_1 reads

$$\begin{aligned}\Theta_1 &= \frac{\theta_a + \theta_\Gamma - \theta_\Gamma^{\text{as}}}{2}, \\ \theta_a &= \arg\left(\frac{B_{12}^{(0)}}{N_1^0}\right) + \frac{\pi}{2}, \\ \theta_\Gamma &= \arg\Gamma(1 + \nu), \quad \theta_\Gamma^{\text{as}} = |\nu| - |\nu| \ln |\nu| - \frac{\pi}{4}.\end{aligned}\tag{59}$$

where $\Gamma(1 + \nu)$ is Euler's gamma function [28].

We note that formula (52) from [28] contains a misprint, however (93) and comments between (92) and (93) are correct.

5.2 Transfer Matrices \mathcal{T}^0 and \mathcal{T}

To apply the transfer matrix (57), we first determine the eigenvalues and eigenfunctions of the unperturbed problem (51). A straightforward calculation gives

$$\beta_j^0(x) = (-1)^j \operatorname{sgn}(x - \varkappa_\varepsilon) \sqrt{(U(x) - U(\varkappa_\varepsilon))^2 - (A_y(x) - A_y(\varkappa_\varepsilon))^2},\tag{60}$$

$$\varphi_j^0(x) = \left(\frac{\beta_j^0(x) - i(A_y(x) - A_y(\varkappa_\varepsilon))}{\varepsilon - U(x)} \right) \frac{1}{x - \varkappa_\varepsilon}.\tag{61}$$

Here, $\varphi_j^0(x)$ is defined up to a scalar function of x , which we choose as $\frac{1}{x - \varkappa_\varepsilon}$ to ensure a finite limit as $x \rightarrow \varkappa_\varepsilon$. The eigenvalue indices are assigned consistently with their behavior near $x = \varkappa_\varepsilon$, see (52).

Near $x \rightarrow \varkappa_\varepsilon$, using

$$\varepsilon - U(x) \approx -U'(\varkappa_\varepsilon)(x - \varkappa_\varepsilon), \quad A_y(x) - A_y(\varkappa_\varepsilon) \approx B(\varkappa_\varepsilon)(x - \varkappa_\varepsilon),\tag{62}$$

we obtain

$$\beta_j^0(x) = (-1)^j Q(\varkappa_\varepsilon)(x - \varkappa_\varepsilon) + o(x - \varkappa_\varepsilon),\tag{63}$$

$$Q(\varkappa_\varepsilon) = \sqrt{(U'(\varkappa_\varepsilon))^2 - B^2(\varkappa_\varepsilon)},\tag{64}$$

$$\varphi_j^0(\varkappa_\varepsilon) = \left(\frac{(-1)^j Q(\varkappa_\varepsilon) - iB(\varkappa_\varepsilon)}{-U'(\varkappa_\varepsilon)} \right) + \dots\tag{65}$$

The vectors $\varphi_j^0(\varkappa_\varepsilon)$, $j = 1, 2$, are linearly independent and smooth in x , fulfilling all conditions required for the application of the transfer matrix formalism from [28].

For comparison of Ψ_j^c with the simplified semiclassical solutions used in the definition of \mathcal{T}^0 , we expand

$$\mathcal{P}(x) = A_y(x) - A_y(\varkappa_\varepsilon) + \sqrt{\hbar} \mathcal{P}_\varepsilon \approx B(\varkappa_\varepsilon)(x - \varkappa_\varepsilon) + \sqrt{\hbar} \mathcal{P}_\varepsilon.\tag{66}$$

Outside the classically allowed region, $|x - \varkappa_\varepsilon| \geq \hbar^{1/2 - \alpha'}$ with $0 < \alpha' < 1/6$ [28], the term $\sqrt{\hbar} \mathcal{P}_\varepsilon$ can be neglected at leading order in \hbar , giving

$$\beta_j \approx \beta_j^0, \quad \frac{\varphi_j(x)}{|N_j(x)|^{1/2}} \approx \operatorname{sign}(x - \varkappa_\varepsilon) \frac{\varphi_j^0(x)}{|N_j^0(x)|^{1/2}}, \quad \gamma_j(x) \approx \gamma_j^0(x),\tag{67}$$

where, according to (24),

$$\gamma_j^0(x) = \frac{(-1)^{j+1}}{2} \operatorname{sign}(x - \varkappa_\varepsilon) \arcsin \frac{A_y(x) - A_y(\varkappa_\varepsilon)}{|U(x) - U(\varkappa_\varepsilon)|}\tag{68}$$

and

$$-\int_{\varkappa_c}^x \operatorname{Im} S_j^0(x') dx' = -\gamma_j^0(x) + \gamma_j^0(\varkappa_c).\tag{69}$$

At the lower integration limit,

$$\arcsin \frac{A_y(x) - A_y(\varkappa_\varepsilon)}{|\varepsilon - U(x)|} \Big|_{x=\varkappa_c} \approx \arcsin \frac{B(\varkappa_\varepsilon)}{|U'(\varkappa_\varepsilon)|} \operatorname{sgn}(\varkappa_c - \varkappa_\varepsilon).\tag{70}$$

Finally, the semiclassical solutions can be written as

$$\Psi_j^{c,0}(x) = \frac{\varphi_j^0(x)}{|N_j^0(x)|^{1/2}} \cdot \exp \left\{ i(-1)^j \operatorname{sgn}(x - \varkappa_\varepsilon) \left[\int_{\varkappa_c}^x \frac{|\beta_j^0(x')|}{\hbar} dx' + \frac{1}{2} \arcsin \frac{A_y(x) - A_y(\varkappa_\varepsilon)}{|U(x) - U(\varkappa_\varepsilon)|} \right] + i\gamma_j^0(\varkappa_c) \right\}, \quad (71)$$

where

$$\gamma_j^0(\varkappa_c) = (-1)^{j+1} \chi_\varepsilon^0, \quad \chi_\varepsilon^0 = \frac{1}{2} \arcsin \frac{B(\varkappa_\varepsilon)}{|U'(\varkappa_\varepsilon)|}. \quad (72)$$

The leading-order relation between solutions with and without the zero superscript is

$$\Psi_j^c(x) \approx \operatorname{sgn}(x - \varkappa_\varepsilon) \Psi_j^{c,0}(x) \exp \left[i(-1)^j (\chi_\varepsilon^0 - \operatorname{sgn}(x - \varkappa_\varepsilon) \chi_\varepsilon) \right], \quad c = \pm, \quad (73)$$

see (72), (26), (19). Consequently, the semiclassical solutions differ solely by a sign—stemming from the amplitude in (67)—and by a constant phase factor, which reflects the choice of the lower integration limit in the Berry phase.

The transfer matrix \mathcal{T}^0 , defined in (57), is expressed in terms of the parameters ν and Θ_1 . Using (65) and (49), we calculate

$$\mathcal{B}_{12}^{(0)} = -2i\mathcal{P}_\varepsilon U'(\varkappa_\varepsilon)(-Q(\varkappa_\varepsilon) + iB(\varkappa_\varepsilon)), \quad N_1^{(0)} = 2Q(\varkappa_\varepsilon)U'(\varkappa_\varepsilon), \quad N_2^{(0)} = -N_1^{(0)}, \quad (74)$$

$$\frac{\mathcal{B}_{12}^{(0)}}{N_1^{(0)}} = i\mathcal{P}_\varepsilon \left(1 - \frac{iB(\varkappa_\varepsilon)}{Q(\varkappa_\varepsilon)} \right), \quad \mathcal{B}_{21}^{(0)} = \overline{\mathcal{B}_{12}^{(0)}}. \quad (75)$$

The controlling parameter ν is

$$\nu = -i \frac{(p_y + A_y(\varkappa_\varepsilon))^2}{2\hbar|U'(\varkappa_\varepsilon)|} \frac{1}{(1 - (B(\varkappa_\varepsilon)/|U'(\varkappa_\varepsilon)|)^2)^{3/2}}. \quad (76)$$

The phase factor Θ_1 reads

$$\Theta_1 = (\chi_\varepsilon - \chi_\varepsilon^0) + \frac{1}{2} \left(\frac{\pi}{2} + \vartheta_\Gamma - \vartheta_\Gamma^{as} \right), \quad (77)$$

with χ_ε and χ_ε^0 defined in (26), (72).

Finally, the transfer matrix \mathcal{T} is written as

$$\mathcal{T} = - \begin{pmatrix} e^{-2i\chi_\varepsilon} \mathcal{T}_{11}^0 & e^{2i\chi_\varepsilon^0} \mathcal{T}_{12}^0 \\ e^{-2i\chi_\varepsilon^0} \mathcal{T}_{21}^0 & e^{2i\chi_\varepsilon} \mathcal{T}_{22}^0 \end{pmatrix}. \quad (78)$$

6 Reflection and Transmission

6.1 Single n - p and p - n junctions

The reflection and transmission coefficients are expressed in terms of the entries of the transfer matrix $\mathcal{T}_{n-p} = \mathcal{T}$ (see (40) and (29)). Using (78), we obtain

$$\begin{aligned} r_{n-p} &= e^{-2i(\chi_\varepsilon^0 + \chi_\varepsilon)} r_{n-p}^0, & r_{n-p}^0 &= -\frac{\mathcal{T}_{21}^0}{\mathcal{T}_{22}^0}, \\ t_{n-p} &= -e^{-2i\chi_\varepsilon} t_{n-p}^0, & t_{n-p}^0 &= \frac{1}{\mathcal{T}_{22}^0}, \end{aligned} \quad (79)$$

where $\mathcal{T}_{n-p}^0 = \mathcal{T}^0$ and $\det \mathcal{T}_{n-p}^0 = 1$.

Equations (79) and (57) yield

$$r_{n-p}^0 = -e^{-2i\Theta_1} \sqrt{1 - e^{-2\pi|\nu|}}, \quad t_{n-p}^0 = e^{-\pi|\nu|}. \quad (80)$$

Taking into account (77), we obtain

$$r_{n-p}^0 = -e^{-2i(\chi_\varepsilon - \chi_\varepsilon^0) - i(\frac{\pi}{2} + \vartheta_\Gamma - \vartheta_\Gamma^{as})} \sqrt{1 - e^{-2\pi|\nu|}}, \quad t_{n-p}^0 = e^{-\pi|\nu|}. \quad (81)$$

Using the relation $e^{-2i\chi_\varepsilon - i\pi/2} = \text{sgn}(\mathcal{P}(\varkappa_\varepsilon))$ for $\mathcal{P}(\varkappa_\varepsilon) \neq 0$, we obtain

$$r_{n-p}^0 = \text{sgn}(p_y + A_y(\varkappa_\varepsilon)) e^{i \arctan\left[\frac{B(\varkappa_\varepsilon)}{Q(\varkappa_\varepsilon)}\right] - i(\vartheta_\Gamma - \vartheta_\Gamma^{as})} \sqrt{1 - e^{-2\pi|\nu|}}. \quad (82)$$

The reflection coefficient changes sign upon reversal of sign of $\mathcal{P}(\varkappa_\varepsilon)$, in agreement with the prediction of [21] for $B = 0$. The solutions $\Psi_j^{c;0}(x)$ remain smooth as functions of $\mathcal{P}(\varkappa_\varepsilon)$. If $\mathcal{P}(\varkappa_\varepsilon) = 0$, then $\nu = 0$ and $r_{n-p}^0 = 0$ according to (82); hence its phase is undefined.

For $|\nu| \gg 1$, we have $\vartheta_\Gamma - \vartheta_\Gamma^{as} \ll 1$, and therefore

$$r_{n-p}^0 \approx \text{sgn}(p_y + A_y(\varkappa_\varepsilon)) e^{i \arctan\left[\frac{B(\varkappa_\varepsilon)}{Q(\varkappa_\varepsilon)}\right]}. \quad (83)$$

In the opposite limit $|\nu| \ll 1$, we have $\vartheta_\Gamma - \vartheta_\Gamma^{as} \approx \pi/4$, and

$$r_{n-p}^0 \approx \sqrt{\frac{\pi}{|U'(\varkappa_\varepsilon)|}} \frac{\mathcal{P}_\varepsilon}{(1 - (B(\varkappa_\varepsilon)/U'(\varkappa_\varepsilon))^2)^{3/4}} e^{i \arctan\left[\frac{B(\varkappa_\varepsilon)}{Q(\varkappa_\varepsilon)}\right] - i\pi/4}, \quad \mathcal{P}_\varepsilon \equiv \frac{\mathcal{P}(\varkappa_\varepsilon)}{\sqrt{\hbar}}, \quad (84)$$

where we used (76) for ν and the definition of \mathcal{P}_ε , see equations (48) and (53). By substituting (81) into (79), we obtain

$$r_{n-p} = e^{-i(\frac{\pi}{2} + \vartheta_\Gamma - \vartheta_\Gamma^{as})} \sqrt{1 - e^{-2\pi|\nu|}}, \quad t_{n-p} = -e^{-i\frac{\pi}{2} \text{sgn} \mathcal{P}_\varepsilon} e^{-\pi|\nu|}, \quad (85)$$

where we used $e^{-4i\chi_\varepsilon} = -1$, as it follows from (26). For $\nu = 0$, $t_{n-p} = -1$, since the right-moving semiclassical solutions acquire a sign change when crossing \varkappa_ε (equations (73), (35)).

Reflection and transmission coefficients from the p - n junction are determined in (42). We take into account that $\mathcal{T}_{p-n} = \tilde{\mathcal{T}}$, $\det \tilde{\mathcal{T}} = 1$. The matrix $\tilde{\mathcal{T}}^0$ is determined by the formula (57) where in the definitions of ν and Θ_1 given in (76) and (77), \varkappa_ε is replaced by $\tilde{\varkappa}_\varepsilon$. Equation (78), where χ_ε^0 and χ_ε are replaced with $\tilde{\chi}_\varepsilon^0$ and $\tilde{\chi}_\varepsilon$, expresses $\tilde{\mathcal{T}}$ through $\tilde{\mathcal{T}}^0$. We get

$$\begin{aligned} r_{p-n} &= e^{2i(\tilde{\chi}_\varepsilon^0 + \tilde{\chi}_\varepsilon)} r_{p-n}^0, & r_{p-n}^0 &= -\frac{\tilde{\mathcal{T}}_{12}^0}{\tilde{\mathcal{T}}_{11}^0}, \\ t_{p-n} &= -e^{2i\tilde{\chi}_\varepsilon} t_{p-n}^0, & t_{p-n}^0 &= \frac{1}{\tilde{\mathcal{T}}_{11}^0}. \end{aligned} \quad (86)$$

Denoting ν , ϑ_Γ , ϑ_Γ^{as} , calculated using $\tilde{\varkappa}_\varepsilon$, with the tilde symbol, we obtain

$$\begin{aligned} r_{p-n}^0 &= -e^{2i(\tilde{\chi}_\varepsilon - \tilde{\chi}_\varepsilon^0) + i(\frac{\pi}{2} + \tilde{\vartheta}_\Gamma - \tilde{\vartheta}_\Gamma^{as})} \sqrt{1 - e^{-2\pi|\tilde{\nu}|}}, & t_{p-n}^0 &= e^{-\pi|\tilde{\nu}|}, \\ r_{p-n} &= e^{i(\frac{\pi}{2} + \tilde{\vartheta}_\Gamma - \tilde{\vartheta}_\Gamma^{as})} \sqrt{1 - e^{-2\pi|\tilde{\nu}|}}, & t_{p-n} &= -e^{i\frac{\pi}{2} \text{sgn} \tilde{\mathcal{P}}_\varepsilon} e^{-\pi|\tilde{\nu}|}. \end{aligned} \quad (87)$$

The transmission coefficients for a single n - p or p - n interface are controlled by the parameter ν (or $\tilde{\nu}$). Using (31), perfect transmission occurs for incidence at the angle $\theta_0(\mathcal{E})$ defined by

$$\sin \theta_0 \equiv -\frac{A_y(\varkappa_\varepsilon)}{\mathcal{E}}, \quad (88)$$

assuming θ_0 is real. In this case

$$\nu = -i \frac{\mathcal{E}^2}{2\hbar|U'(\varkappa_\varepsilon)|} (\sin \theta - \sin \theta_0)^2 \left(1 - \left(\frac{B(\varkappa_\varepsilon)}{U'(\varkappa_\varepsilon)}\right)^2\right)^{-3/2}. \quad (89)$$

In the semiclassical regime $\mathcal{E}^2/(2\hbar|U'|) \gg 1$, transmission is confined to $|\theta - \theta_0| \ll 1$. Expanding (89) to leading order in $\theta - \theta_0$, we obtain

$$\nu \approx -i \frac{\mathcal{E}^2}{2\hbar|U'(\varkappa_\varepsilon)|} (\theta - \theta_0)^2 \frac{1 - \left(\frac{\int_{x_*}^{\varkappa_\varepsilon} B(\tilde{x}) d\tilde{x}}{\int_{x_*}^{\varkappa_\varepsilon} U'(\tilde{x}) d\tilde{x}}\right)^2}{\left(1 - \left(\frac{B(\varkappa_\varepsilon)}{U'(\varkappa_\varepsilon)}\right)^2\right)^{3/2}}. \quad (90)$$

6.2 Fabry–Pérot resonances

To evaluate the transmission coefficient through an n - p - n junction using (46), we express the transfer matrix of the n - p - n structure (see (45)) in terms of the reflection and transmission coefficients of the n - p and p - n junctions. The corresponding transfer matrices \mathcal{T}_{n-p} and \mathcal{T}_{p-n} can be written as

$$\mathcal{T}_{n-p} = \begin{pmatrix} 1/\overline{t_{n-p}} & -\overline{r_{n-p}}/\overline{t_{n-p}} \\ -r_{n-p}/t_{n-p} & 1/t_{n-p} \end{pmatrix}, \quad \mathcal{T}_{p-n} = \begin{pmatrix} 1/t_{p-n} & -r_{p-n}/t_{p-n} \\ -\overline{r_{p-n}}/\overline{t_{p-n}} & 1/\overline{t_{p-n}} \end{pmatrix}. \quad (91)$$

These expressions follow from (40) and (42). After straightforward calculations, (46) yields

$$t_{n-p-n} = \frac{|t_{n-p}| |t_{p-n}| e^{-i(\zeta - \arg t_{n-p} - \arg t_{p-n})}}{1 + e^{-2i(\zeta - \arg t_{n-p})} \overline{r_{n-p}} r_{p-n}}. \quad (92)$$

The Fabry–Pérot resonances are determined by the condition

$$1 + e^{-2i(\zeta - \arg t_{n-p})} \overline{r_{n-p}} r_{p-n} = 0. \quad (93)$$

Substituting into (93) the expressions for ζ , (43), t_{n-p} and r_{n-p} , see (85), and r_{p-n} , see (87), we obtain

$$\delta(\mathcal{E}, \theta) = 2\pi M + i \ln |r_{n-p} r_{p-n}|, \quad (94)$$

where M is an integer and

$$\delta(\mathcal{E}, \theta) \equiv -\frac{2}{\hbar} \int_{\varkappa_h}^{\tilde{\varkappa}_h} |\beta(x')| dx' - \frac{\pi}{2} (\text{sgn} \mathcal{P}_{\mathcal{E}} + \text{sgn} \tilde{\mathcal{P}}_{\mathcal{E}}) + \vartheta_{\Gamma} - \vartheta_{\Gamma}^{\text{as}} + \tilde{\theta}_{\Gamma} - \tilde{\theta}_{\Gamma}^{\text{as}}. \quad (95)$$

Following [13, 14], we calculate $|t_{n-p-n}|^2$ as a function of the angle of incidence of the charge carrier. Multiplying (92) by its complex conjugate, we find

$$|t_{n-p-n}|^2 = \frac{|t_{n-p} t_{p-n}|^2}{(1 - |r_{n-p} r_{p-n}|)^2 + 4|r_{n-p} r_{p-n}| \sin^2(\delta/2)}. \quad (96)$$

Figure 4 shows the absolute value of t_{n-p-n} as a function of the angle of incidence θ . Equation (96) demonstrates that the transmission probability reaches its maximum when $\delta = 2\pi M$, where M is an integer. The corresponding angles are referred to as “magic” angles [8, 13, 14]. The maximal transmission satisfies $|t_{n-p-n}|_{\text{max}} = 1$ if $|r_{n-p}| = |r_{p-n}|$, therefore suppression of transmission requires an asymmetric barrier. Using (96), we have calculated the transmission probability through the barrier shown in Fig. 1(b) with magnetic-field profiles depicted in Fig. 1(c). Figure 4 presents a polar plot of $|t_{n-p-n}|$ versus the angle of incidence θ . In the absence of a magnetic field [Fig. 4(a)], the positions of the “magic” angles coincide with those reported in [14]. An external magnetic field introduces additional asymmetry, resulting in a shift of the “magic” angle positions. If $U(-x) = U(x)$ and $B(-x) = -B(x)$, full transmission at the “magic” angles remains possible even in the presence of a magnetic field; in this case $A_y(-x) = A_y(x)$ and $\nu(\varkappa_{\mathcal{E}}) = \nu(\tilde{\varkappa}_{\mathcal{E}})$.

We anticipate a qualitative modification of the interference structure along the lines in the (p_y, \mathcal{E}) plane defined by

$$\mathcal{P}(\varkappa_{\mathcal{E}}) = 0, \quad \mathcal{P}(\tilde{\varkappa}_{\mathcal{E}}) = 0, \quad (97)$$

which correspond to

$$p_y^{(1)} = -A_y(\varkappa_{\mathcal{E}}), \quad p_y^{(2)} = -A_y(\tilde{\varkappa}_{\mathcal{E}}), \quad (98)$$

where $|t_{n-p}| = 1$ and $|t_{p-n}| = 1$, respectively. At these lines one of the junctions becomes perfectly transparent, so that the corresponding reflection coefficient vanishes and changes sign upon crossing. As follows from (95), this sign reversal produces a discontinuous jump of the phase δ by π . Since $\delta = 2\pi M$ corresponds to constructive interference and $\delta = (2M + 1)\pi$ to destructive interference, the π phase jump interchanges transmission maxima and minima. Thus, crossing either of these lines in the (p_y, \mathcal{E}) plane results in an abrupt reconfiguration of the interference pattern.

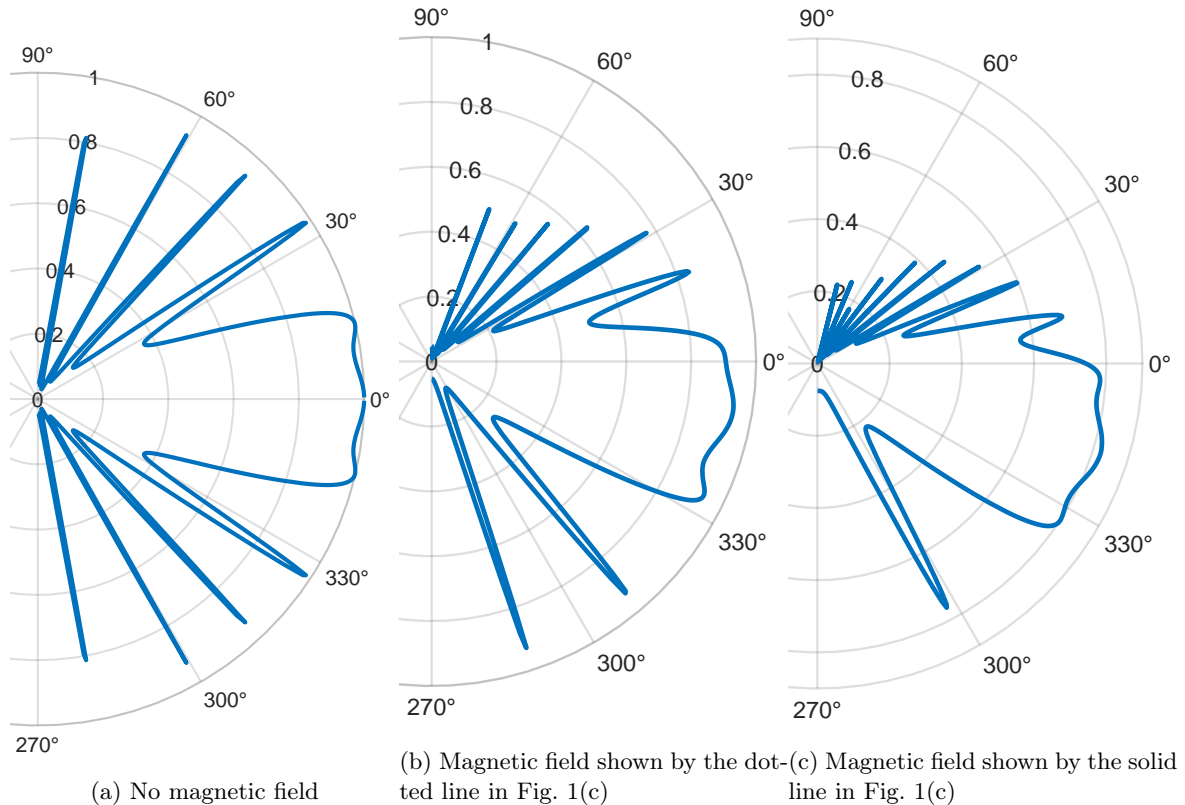


Figure 4: The absolute value of t_{n-p-n} as a function of the angle of incidence on the barrier.

7 Conclusion

In this work, we developed a semiclassical description of fermion tunneling through an inhomogeneous potential barrier in graphene in the presence of an inhomogeneous magnetic field. Both the electrostatic and magnetic fields are assumed to vary smoothly along the transport (x) direction while remaining uniform in the transverse (y) direction. Within this framework, we derived the magnitudes and phases of the reflection and transmission coefficients for $n-p$ and $p-n$ junctions; the corresponding results are given in (85) and (87). In the absence of a magnetic field, our results are consistent with those of [13, 14].

We further analyzed electron transmission through an $n-p-n$ junction. Analytical expressions for the Fabry-Pérot resonances and the so-called “magic” angles were obtained. We predict a restructuring of the interference pattern at angles of incidence and energies corresponding to a complete transition through one of the junctions $n-p$ or $p-n$.

In addition, we performed numerical calculations of the transmission coefficient as a function of the angle of incidence. In the limiting case of a vanishing magnetic field, our results reduce to those reported in [14], demonstrating full agreement.

A Zero-Magnetic-Field Limit

In this Appendix, we compare the semiclassical expressions obtained in the present work for the reflection and transmission coefficients r_{n-p} and t_{n-p} with the results of [13, 14] in the absence of a magnetic field. Specifically, we relate the semiclassical modes given in (35),(25) to the asymptotic scattering states (C.3) and (C.6) of [14].

We adopt the notation $\phi_p^+(x)$ and $v(x)$ introduced in (C.4) of [14]:

$$\cos \phi_p^+(x) = \frac{\beta(x)}{|v(x)|}, \quad \sin \phi_p^+(x) = \frac{\mathcal{P}(x)}{|v(x)|}, \quad U(x) - \mathcal{E} = v(x). \quad (99)$$

Here $\beta(x)$ is defined in (16) and satisfies $\beta(x) > 0$. It follows that

$$\beta^2(x) + \mathcal{P}^2(x) = v^2(x), \quad \sqrt{\beta^2(x) + \mathcal{P}^2(x)} = |v(x)|. \quad (100)$$

Consequently,

$$\begin{aligned}\phi_p^+(x) &= \arcsin \frac{\mathcal{P}(x)}{|\mathcal{E} - U(x)|}, \\ \beta(x) \mp i\mathcal{P}(x) &= |v(x)|e^{\mp i\phi_p^+(x)}.\end{aligned}\tag{101}$$

In the electron region, where $|v(x)| = -v(x)$, the semiclassical solutions (25), (35) take the form

$$\Psi_{eR}(x) = \frac{|v(x)|}{|2\beta v(x)|^{1/2}} \begin{pmatrix} e^{-\frac{i}{2}\phi_p^+(x)} \\ e^{\frac{i}{2}\phi_p^+(x)} \end{pmatrix} e^{i \int_{\varkappa_e}^x \frac{\beta(x')}{\hbar} dx' - i\frac{\pi}{4} \text{sgn}\mathcal{P}(\varkappa_{\mathcal{E}})},\tag{102}$$

$$\Psi_{eL}(x) = \frac{|v(x)|}{|2\beta v(x)|^{1/2}} \begin{pmatrix} -e^{\frac{i}{2}\phi_p^+(x)} \\ e^{-\frac{i}{2}\phi_p^+(x)} \end{pmatrix} e^{-i \int_{\varkappa_e}^x \frac{\beta(x')}{\hbar} dx' + i\frac{\pi}{4} \text{sgn}\mathcal{P}(\varkappa_{\mathcal{E}})}.\tag{103}$$

In the hole region, where $|v(x)| = v(x)$, one obtains

$$\Psi_{hR}(x) = -\frac{|v(x)|}{|2\beta v(x)|^{1/2}} \begin{pmatrix} e^{\frac{i}{2}\phi_p^+(x)} \\ e^{-\frac{i}{2}\phi_p^+(x)} \end{pmatrix} e^{-i \int_{\varkappa_e}^x \frac{\beta(x')}{\hbar} dx' + i\frac{\pi}{4} \text{sgn}\mathcal{P}(\varkappa_{\mathcal{E}})},\tag{104}$$

$$\Psi_{hL}(x) = \frac{|v(x)|}{|2\beta v(x)|^{1/2}} \begin{pmatrix} e^{-\frac{i}{2}\phi_p^+(x)} \\ -e^{\frac{i}{2}\phi_p^+(x)} \end{pmatrix} e^{i \int_{\varkappa_e}^x \frac{\beta(x')}{\hbar} dx' - i\frac{\pi}{4} \text{sgn}\mathcal{P}(\varkappa_{\mathcal{E}})}.\tag{105}$$

In the absence of a magnetic field, $\mathcal{P}(x) = p_y$ and $\text{sgn}\mathcal{P}(\varkappa_{\mathcal{E}}) = \text{sgn}p_y$. For small p_y changing sign, the semiclassical modes Ψ_{ec} , Ψ_{hc} , $c = R, L$ exhibit a sharp variation due to the phase terms proportional to $\text{sgn}p_y$.

We denote the semiclassical modes of [14] by $\Psi_{\pm}^{\text{RTK}}(x)$. In that work, the phase $\phi_p^-(x)$ is defined such that

$$\phi_p^+(x) = \pi \text{sgn}p_y - \phi_p^-(x),\tag{106}$$

which implies

$$\begin{aligned}-e^{\frac{i}{2}\phi_p^+(x)} &= -e^{i\frac{\pi}{2}\text{sgn}p_y} e^{-\frac{i}{2}\phi_p^-(x)}, \\ e^{-\frac{i}{2}\phi_p^+(x)} &= e^{-i\frac{\pi}{2}\text{sgn}p_y} e^{\frac{i}{2}\phi_p^-(x)}.\end{aligned}\tag{107}$$

For $p_y \neq 0$ and $x_0 = \varkappa_e$, the electron-region solutions are related by

$$\Psi_{+}^{\text{RTK}}(x) = e^{i\frac{\pi}{4}\text{sgn}p_y} \frac{2}{\sqrt{|p_y|}} \Psi_{eR}(x), \quad \Psi_{-}^{\text{RTK}}(x) = e^{i\frac{\pi}{4}\text{sgn}p_y} \frac{2}{\sqrt{|p_y|}} \Psi_{eL}(x).\tag{108}$$

The reflection coefficient r_{n-p} defined in (85) coincides with the reflection coefficient r of [14], given in (69) and (73) therein. The correspondence between parameters is

$$\nu = -i\frac{K}{\pi\hbar}, \quad \vartheta_{\Gamma} - \vartheta_{\Gamma}^{\text{as}} = -\theta.\tag{109}$$

The hole-region solutions (C.6) of [14] and solutions (104), (105) are related by

$$\Psi_{+}^{\text{RTK}}(x) = e^{i\frac{3\pi}{4}\text{sgn}p_y} \frac{2}{\sqrt{|p_y|}} \Psi_{hL}(x), \quad \Psi_{-}^{\text{RTK}}(x) = e^{i\frac{3\pi}{4}\text{sgn}p_y} \frac{2}{\sqrt{|p_y|}} \Psi_{hR}(x).\tag{110}$$

This holds if equation (C.6) involves $S(x_0, x)$ rather than $S(x, x_0)$. Then, the transition coefficient t from [14] (equation (62)) is related to t_{n-p} , as dictated by (110) and (108), i.e., $t = -e^{i\frac{\pi}{2}\text{sgn}p_y} t_{n-p}$.

References

- [1] K S Novoselov, A K Geim, S V Morozov, D Jiang, Y Zhang, S V Dubonos, I V Grigorieva, and A A Firsov. Electric field effect in atomically thin carbon films. *Science*, 306(5696):666–669, 2004.
- [2] K. S. Novoselov, A. K. Geim, S. V. Morozov, D. Jiang, M. I. Katsnelson, I. V. Grigorieva, S. V. Dubonos, and A. A. Firsov. Two-dimensional gas of massless dirac fermions in graphene. *Nature*, 438(7065):197–200, 2005.

- [3] A H Castro Neto, F Guinea, N M R Peres, K S Novoselov, and A K Geim. The electronic properties of graphene. *Reviews of Modern Physics*, 81(1):109–162, 2009.
- [4] M. I. Katsnelson. Graphene: carbon in two dimensions. *Materials Today*, 10(1-2):20–27, 2007.
- [5] C W J Beenakker. Colloquium: Andreev reflection and Klein tunneling in graphene. *Reviews of Modern Physics*, 80(4):1337–1354, 2008.
- [6] A. C. Ferrari, F. Bonaccorso, V. Fal’Ko, K. S. Novoselov, S. Roche, P. Bøggild, S. Borini, F. H. L. Koppens, V. Palermo, and N. Pugno. Science and technology roadmap for graphene, related two-dimensional crystals, and hybrid systems. *Nanoscale*, 7(11):4598–4810, 2015.
- [7] M. I. Katsnelson. *The physics of graphene*. Cambridge University Press, 2020.
- [8] M. I. Katsnelson, K. S. Novoselov, and A. K. Geim. Chiral tunnelling and the Klein paradox in graphene. *Nature Physics*, 2(9):620–625, 2006.
- [9] O. Klein. Die reflexion von elektronen an einem potentialsprung nach der relativistischen dynamik von Dirac. *Zeitschrift für Physik*, 53(3):157–165, 1929.
- [10] V. V. Cheianov and V. I. Fal’ko. Selective transmission of Dirac electrons and ballistic magnetoresistance of n-p junctions in graphene. *Physical Review B*, 74(4):041403, 2006.
- [11] E. B. Sonin. Effect of Klein tunneling on conductance and shot noise in ballistic graphene. *Physical Review B*, 79(19):195438, 2009.
- [12] R R Hartmann, N J Robinson, and M E Portnoi. Smooth electron waveguides in graphene. *Physical Review B*, 81(24):245431, 2010.
- [13] T. Tudorovskiy, K. J. A. Reijnders, and M. I. Katsnelson. Chiral tunneling in single-layer and bilayer graphene. *Physica Scripta*, T146:014010, 2012.
- [14] K. J. A. Reijnders, T. Tudorovskiy, and M. I. Katsnelson. Semiclassical theory of potential scattering for massless Dirac fermions. *Annals of Physics*, 333:155–197, 2013.
- [15] V. Zalipaev, C. M. Linton, M. D. Croitoru, and A. Vagov. Resonant tunneling and localized states in a graphene monolayer with a mass gap. *Physical Review B*, 91(8):085405, 2015.
- [16] A. De Martino, L. Dell’Anna, and R. Egger. Magnetic barriers and confinement of Dirac-Weyl quasiparticles in graphene. *Solid State Communications*, 144:547–550, 2007.
- [17] L. Dell’Anna and A. De Martino. Multiple magnetic barriers in graphene. *Physical Review B*, 79:045420, 2009.
- [18] C. A. Downing and M. E. Portnoi. Massless Dirac fermions in two dimensions: Confinement in nonuniform magnetic fields. *Physical Review B*, 94(16):165407, 2016.
- [19] A. V. Shytov, N. Gu, and L. S. Levitov. Transport in graphene pn junctions in magnetic field. *arXiv*, 2007.
- [20] A. Shytov, M. Rudner, N. Gu, M. Katsnelson, and L. Levitov. Atomic collapse, Lorentz boosts, Klein scattering, and other quantum-relativistic phenomena in graphene. *Solid State Communications*, 149(27-28):1087–1093, 2009.
- [21] A. V. Shytov, M. S. Rudner, and L. S. Levitov. Klein backscattering and Fabry-Pérot interference in graphene heterojunctions. *Physical Review Letters*, 101(15):156804, 2008.
- [22] M. R. Masir, P. Vasilopoulos, and F. M. Peeters. Fabry-Pérot resonances in graphene microstructures: Influence of a magnetic field. *Physical Review B*, 82(11):115417, 2010.
- [23] M. Mekkaoui, A. Jellal, and H. Bahlouli. Tunneling of electrons in graphene via double triangular barrier in external fields. *Solid State Communications*, 358:114981, 2022.
- [24] Z. Kong, J. Li, Y. Zhang, S.-H. Zhang, and J.-J. Zhu. Oblique and asymmetric Klein tunneling across smooth np junctions or npn junctions in 8-pmmn borophene. *Nanomaterials*, 11(6):1462, 2021.

- [25] P Carmier, C H Lewenkopf, and D Ullmo. Semiclassical magnetotransport in graphene n-p junctions. *Physical Review B*, 84(19):195428, 2011.
- [26] M. V. Perel. Overexcitation of modes in an anisotropic earth-ionosphere waveguide on transequatorial paths in the presence of two close degeneracy points. *Radiophysics and Quantum Electronics*, 33(11):882–889, 1990.
- [27] Maria V Perel, Julius D Kaplunov, and Graham A Rogerson. An asymptotic theory for internal reflection in weakly inhomogeneous elastic waveguides. *Wave motion*, 41(2):95–108, 2005.
- [28] I. Fialkovsky and M. Perel. Mode transformation for a Schrödinger type equation: avoided and unavoidable level crossings. *Journal of Mathematical Physics*, 61(4):043506, 2020.
- [29] L D Landau. Diamagnetismus der metalle. *Zeitschrift für Physik*, 64:629–637, 1930.
- [30] M. V. Berry and K. E. Mount. Semiclassical approximations in wave mechanics. *Reports on Progress in Physics*, 35(1):315–397, 1972.
- [31] L. D. Landau and E. M. Lifshitz. *Quantum mechanics: Non-relativistic theory*, volume 3. Elsevier, 2013.
- [32] M. V. Fedoryuk. *Asymptotic analysis: linear ordinary differential equations*. Springer Science & Business Media, 2012.
- [33] V. P. Maslov and M. V. Fedoriuk. *Semi-classical approximation in quantum mechanics*, volume 7. Springer, 2001.